

Influence of Side Chains on Electronic Coupling between Metal Centers in Simple Model Systems

Nita A. Lewis* and Wei Pan

Department of Chemistry, University of Miami, Coral Gables, Florida 33124

Received June 22, 1994[⊗]

Studies on both small and large molecules, especially proteins, have been reported in which the electron transfer pathways are better described by a through-bond than a direct metal-to-metal distance. The role of the intervening matter in the redox process is difficult to quantify. In the present study, the through-bond distance and driving force between the donor and acceptor are constant in a series of binuclear complexes and only the side chains along the electron transfer pathway are changed in a systematic manner. Correlations are observed between functions of E_{op} and ϵ_{max} of the transition bands and $\Delta E_{1/2}$ measured electrochemically, the sum of the Taft σ_1 parameters for the substituents, the dihedral angle between the two pseudoaromatic rings in the system, and the HOMO bond energies of the complexes calculated by ZINDO.

Introduction

Electron transfer reactions are fundamentally important to most areas of industrial endeavors as well as to all biological organisms. During the past decade, a substantial effort has been put forth to attempt to understand the complexities of this process in redox proteins where the metal center is usually buried in the interior of the molecule.¹ The theoretical analysis of the results of protein studies is a formidable task although tremendous progress has been made and new tools have been

developed specifically for the quantum electronic analysis of the inhomogeneous, three-dimensional aperiodic nature of the protein structures.² These tools rely heavily on the lessons learned from an analysis of the electron transfer reactions in small model compounds.³ Originally, it was thought that the factors that controlled the rate of electron transfer were the driving force, reorganization energy, and distance between the reacting centers. It is now generally believed that the nature

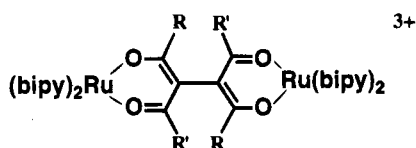
[⊗] Abstract published in *Advance ACS Abstracts*, March 15, 1995.

- (1) (a) Winkler, J. R.; Nocera, D. G.; Yokum, K. M.; Bordignon, E.; Gray, H. B. *J. Am. Chem. Soc.* **1982**, *104*, 5798. (b) Yokum, K. M.; Shelton, J. B.; Shelton, J. R.; Schroeder, W. A.; Worosila, G.; Isied, S. S.; Bordignon, E.; Gray, H. B. *Proc. Natl. Acad. Sci. U.S.A.* **1982**, *79*, 7052. (c) Yokum, K. M.; Winkler, J. R.; Nocera, D. G.; Bordignon, E.; Gray, H. B. *Chem. Scr.* **1983**, *21*, 29. (d) Kostic, N. M.; Margalit, R.; Che, C.-M.; Gray, H. B. *J. Am. Chem. Soc.* **1983**, *105*, 7765. (e) Margalit, R.; Pecht, I.; Gray, H. B. *J. Am. Chem. Soc.* **1983**, *105*, 301. (f) Nocera, D. G.; Winkler, J. R.; Yokum, K. M.; Bordignon, E.; Gray, H. B. *J. Am. Chem. Soc.* **1984**, *106*, 5145. (g) Toi, H.; La Mar, G. N.; Margalit, R.; Che, C.-M.; Gray, H. B. *J. Am. Chem. Soc.* **1984**, *106*, 6213. (h) Margalit, R.; Kostic, N. M.; Che, C.-M.; Blair, D. F.; Chiang, H.; Pecht, I.; Shelton, J. B.; Shelton, W. A.; Gray, H. B. *Proc. Natl. Acad. Sci. U.S.A.* **1984**, *81*, 6554. (i) Crutchley, R. J.; Ellis, W. R., Jr.; Gray, H. B. *J. Am. Chem. Soc.* **1985**, *107*, 5002. (j) Scott, R. A.; Mauk, A. G.; Gray, H. B. *J. Chem. Educ.* **1985**, *62*, 932. (k) Crutchley, R. J.; Ellis, W. R., Jr.; Gray, H. B. *Front. Bioinorg. Chem.* **1986**, *2*, 679. (l) Wuttke, D. S.; Bjerrum, M. J.; Chang, I.-J.; Winkler, J. R.; Gray, H. B. *Biochim. Biophys. Acta* **1992**, *1101*, 168. (m) Wuttke, D. S.; Bjerrum, M. J.; Winkler, J. R.; Gray, H. B. *Science* **1992**, *256*, 1007. (n) Mayo, S. L.; Ellis, W. R., Jr.; Crutchley, R. J.; Gray, H. B. *Science* **1986**, *233*, 948. (o) Therein, M. J.; Selman, M.; Gray, H. B.; Chang, I.-J.; Winkler, J. R. *J. Am. Chem. Soc.* **1990**, *112*, 2420. (p) Casimiro, D. R.; Wong, L.-L.; Colon, J. L.; Zewert, T. E.; Richards, J. H.; Chang, I.-J.; Winkler, J. R.; Gray, H. B. *J. Am. Chem. Soc.* **1993**, *115*, 1485. (q) McLendon, G. *Acc. Chem. Res.* **1988**, *21*, 160. (r) Liang, N.; Pielak, G.; Mauk, A. G.; Smith, M.; Hoffman, B. M. *Proc. Natl. Acad. Sci. U.S.A.* **1987**, *84*, 1249. (s) Liang, N.; Mauk, A. G.; Pielak, G. L.; Johnson, J. A.; Smith, M.; Hoffman, B. M. *Science* **1988**, *240*, 311. (t) Everest, A. M.; Wallin, S. A.; Stemp, E. D. A.; Nocek, J. M.; Mauk, A. G.; Hoffman, B. M. *J. Am. Chem. Soc.* **1991**, *113*, 4337. (u) Hoffman, B. M.; Natan, M. J.; Nocek, J. M.; Wallin, S. A. *Biology, Structure and Bonding*, 75; Springer-Verlag: Berlin, 1991; pp 85–108. (v) Bowler, B. E.; Raphael, A. L.; Gray, H. B. *Prog. Inorg. Chem. Bioinorg. Chem.* **1990**, *38*, 259. (w) Lowery, M. D.; Guckert, J. A.; Gebhard, M. S.; Solomon, E. I. *J. Am. Chem. Soc.* **1993**, *115*, 3012. (x) Axup, A. W.; Albin, M.; Mayo, S. L.; Crutchley, R. L.; Gray, H. B. *J. Am. Chem. Soc.* **1988**, *110*, 435. (y) Scott, J. R.; Willie, A.; McLean, M.; Stayton, P. S.; Sliagar, S. G.; Durham, B.; Millett, F. *J. Am. Chem. Soc.* **1993**, *115*, 6820. (z) Winkler, J. R.; Gray, H. B. *Chem. Rev.* **1992**, *92*, 369.

- (2) (a) Beratan, D. N.; Onuchic, J. N.; Winkler, J. R.; Gray, H. B. *Science* **1992**, *258*, 1740. (b) Beratan, D. N.; Onuchic, J. N.; Hopfield, J. J. *J. Chem. Phys.* **1987**, *86*, 4488. (c) Beratan, D. N.; Onuchic, J. N. *Photosynth. Res.* **1989**, *22*, 173. (d) Beratan, D. N.; Onuchic, J. N.; Betts, J. N.; Bowler, B. E.; Gray, H. B. *J. Am. Chem. Soc.* **1990**, *112*, 7915. (e) Onuchic, J. N.; Beratan, D. N. *J. Phys. Chem.* **1990**, *92*, 722. (f) Onuchic, J. N.; Andrade, P. C. P.; Beratan, D. N. *J. Chem. Phys.* **1991**, *95*, 1131. (g) Beratan, D. N.; Betts, J. N.; Onuchic, J. N. *J. Phys. Chem.* **1992**, *96*, 2852. (h) Betts, J. N.; Beratan, D. N.; Onuchic, J. N. *J. Am. Chem. Soc.* **1992**, *114*, 4043. (i) Kuki, A.; Wolynes, P. G. *Science* **1987**, *236*, 1647. (j) Onuchic, J. N.; Beratan, D. N. *J. Am. Chem. Soc.* **1987**, *109*, 6771.
- (3) (a) Lewis, N. A.; Obeng, Y. S. *J. Am. Chem. Soc.* **1988**, *110*, 2306. (b) Lewis, N. A.; Obeng, Y. S. *J. Am. Chem. Soc.* **1989**, *111*, 7624. (c) Stein, C. A.; Lewis, N. A.; Seitz, G. J. *J. Am. Chem. Soc.* **1982**, *104*, 2596. (d) Stein, C. A.; Lewis, N. A.; Baker, A. D.; Seitz, G. *Inorg. Chem.* **1983**, *22*, 1124. (e) Lewis, N. A.; Obeng, S.; Purcell, W. L. *Inorg. Chem.* **1989**, *28*, 3796. (f) Sutin, N. *Acc. Chem. Res.* **1982**, *15*, 275. (g) Sutin, N. *Prog. Inorg. Chem.* **1983**, *30*, 441. (h) Wherland, S.; Gray, H. B. In *Biological Aspects of Inorganic Chemistry*; Addison, A. W., Cullen, W. R., Dolphin, D., James, B. R., Eds.; Wiley: New York, 1977; pp 289–368. (i) Marcus, R. A. *Annu. Rev. Phys. Chem.* **1964**, *15*, 155. (j) Marcus, R. A. *J. Phys. Chem.* **1956**, *24*, 996. (k) Marcus, R. A.; Sutin, N. *Biochim. Biophys. Acta* **1985**, *811*, 265. (l) Isied, S. S. In *Metal Ions in Biological Systems*; Sigel, H., Sigel, A., Eds.; Marcel Dekker: New York, 1991; Vol. 27, pp 1–56. (m) Vassilian, A.; Wishart, J. F.; van Hemelryck, B.; Schwarz, H.; Isied, S. S. *J. Am. Chem. Soc.* **1990**, *112*, 7278. (n) Isied, S. S.; Vassilian, A. *J. Am. Chem. Soc.* **1994**, *106*, 1732. (o) Isied, S. S.; Vassilian, A.; Magnuson, R.; Schwarz, H. *J. Am. Chem. Soc.* **1985**, *107*, 7432. (p) Isied, S. S.; Ogawa, M. Y.; Wishart, J. F. *Chem. Rev.* **1992**, *92*, 381. (q) Inai, Y.; Sisido, M.; Imanishi, Y. *J. Phys. Chem.* **1990**, *94*, 6237. (r) Inai, Y.; Tamaka, R.; Inai, Y.; Imanishi, Y. *J. Am. Chem. Soc.* **1989**, *111*, 6790. (s) Inai, Y.; Sisido, M.; Imanishi, Y. *J. Phys. Chem.* **1991**, *95*, 3847. (t) Dong, T.-Y.; Hwang, M.-Y.; Wen, Y.; Hwang, W.-S. *J. Organomet. Chem.* **1990**, *391*, 377. (u) Dong, T.-Y.; Huang, C.-H.; Chang, C.-K.; Wen, Y.-S.; Lee, S.-L.; Chen, J.-A.; Yeh, W.-Y.; Yeh, A. *J. Am. Chem. Soc.* **1993**, *115*, 6357. (v) Creutz, C.; Taube, H. *J. Am. Chem. Soc.* **1969**, *91*, 3988. (w) Creutz, C.; Taube, H. *J. Am. Chem. Soc.* **1973**, *95*, 1086. (x) Tom, G. M.; Creutz, C.; Taube, H. *J. Am. Chem. Soc.* **1974**, *96*, 7828. (y) Meyer, T. J. *Acc. Chem. Res.* **1978**, *11*, 94. (z) Meyer, T. J. In *Mixed-valence Compounds*; Brown, D. B., Ed.; NATO Advanced Study Institute Series, No. 58; D. Reidel: Boston, MA, 1980.

of the intervening residues and their orientation relative to the donor and acceptor groups are also important both for small molecules and for proteins. In addition, it has been found that conformational change may be a controlling factor for biological electron transfer.⁴

In the light of these results, our focus in the present work is to examine the effect on the rate of electron transfer of a change in side chain along the electronic pathway. We are particularly concerned with determining if benzene rings may enhance the through-space coupling between metal centers in a small model system and, if so, how this may best be incorporated into the theoretical description. In our models, the driving force and through-bond distances are held constant. The side chain is varied systematically from methyl, which presumably cannot be involved in through-space interactions, to phenyl in four positions, giving the series of compounds



These compounds will be abbreviated as shown in the square brackets: $R = R' = \text{CH}_3$ [$\text{RuMe}_2\text{Me}_2\text{Ru}$], $R = \text{CH}_3$, $R' = \text{C}_6\text{H}_5$ [$\text{RuMe}_2\text{Ph}_2\text{Ru}$], and $R = R' = \text{Ph}$ [$\text{RuPh}_2\text{Ph}_2\text{Ru}$]. The corresponding mononuclear derivatives will have similar mnemonics i.e. [RuMe_2Me_2], [RuMe_2Ph_2], and [RuPh_2Ph_2]. An important goal of the present research was to determine if the role of the phenyl groups is mainly steric or if the phenyl groups enhance the rate of electron transfer via additional pathways with contributions from nonbonded interactions between the phenyl groups and the bipyridine rings.

Experimental Section

Physical Measurements. The UV-vis–near-IR measurements were performed on a Perkin-Elmer Lambda 9 spectrophotometer interfaced to an IBM PC/XT microcomputer. Software to run the spectrophotometer is provided commercially by Softways. Cyclic voltammograms were run on a BAS-100 electrochemical analyzer (from Bioanalytical Systems Inc.). The electrochemical cell contained the standard three-electrode arrangement: a Ag/AgCl reference electrode, a Pt wire counter electrode, and a glassy carbon working electrode. All solutions were thoroughly degassed with argon prior to beginning the experiment, and all $E_{1/2}$ values are uncorrected for junction potentials.

Chemicals. The CH_3CN used for cyclic voltammetry and spectrophotometry was spectroscopic grade from Aldrich stored over 4 Å molecular sieves. All solvents employed in the syntheses were reagent grade and were used without further purification. Tetra-*n*-butylammonium hexafluorophosphate (TBAH) was obtained from Aldrich Chemicals and was recrystallized from acetone. Ammonium hexafluorophosphate (NH_4PF_6) was also purchased from Aldrich Chemicals and was used as supplied.

Syntheses. The starting material, *cis*-[(bpy)₂RuCl₂] \cdot 2H₂O, was prepared by the published procedure.⁵ The bridging ligands, 3,4-

diacetyl-2,5-hexanedione, 3,4-dibenzoyl-2,5-hexanedione, and *s*-tetra-benzoyl-ethane, were prepared according to previously published methods.⁶

The mixed-valence compounds, [(bpy)₂RuL Ru(bpy)₂]³⁺, were generated by the oxidation of the fully reduced isovalent species upon the addition of 1 equiv of (NH_4)₂Ce(NO_3)₆. The fully oxidized isovalent species were generated by the addition of a second equivalent of the same oxidizing agent.

Preparation of [(bpy)₂RuL Ru(bpy)₂](PF₆)₂ Dinuclear Compounds. A mixture of *cis*-[(bpy)₂RuCl₂] \cdot 2H₂O (0.200 g, 0.38 mmol), the desired ligand (0.2 mmol), and NaOH (0.016 g, 0.4 mmol) was refluxed in absolute ethanol for 48 h. After the mixture was cooled to room temperature, an excess of solid NH_4PF_6 (ca 0.3 g) was added and the product crystallized upon refrigeration for several hours. The product was collected by vacuum filtration. The compound [$\text{RuMe}_2\text{Me}_2\text{Ru}$] was further purified by column chromatography. A concentrated acetonitrile solution of the crude material was applied to a 60 cm \times 5 cm silica gel column which was taken eluted with 4:1 $\text{CH}_2\text{Cl}_2/\text{CH}_3\text{CN}$. A small amount of the red mononuclear band moved down the column first, followed by the purple dinuclear species. The band containing the dinuclear material was collected and evaporated to dryness under reduced pressure. The product was further purified by recrystallization from 1:5 $\text{CH}_3\text{CN}/\text{CH}_3\text{CH}_2\text{OH}$ and then dried under vacuum. For both compounds [$\text{RuMe}_2\text{Ph}_2\text{Ru}$] and [$\text{RuPh}_2\text{Ph}_2\text{Ru}$], the crude mixtures were subjected to thin-layer rather than column chromatography. The solvent mixture employed was 5:1 $\text{CH}_2\text{Cl}_2/\text{CH}_3\text{CN}$. The purple bands were collected, dissolved in CH_3CN , recrystallized from 1:5 $\text{CH}_3\text{CN}/\text{CH}_3\text{CH}_2\text{OH}$, and dried under vacuum. Anal. Calc for $\text{C}_{50}\text{H}_{44}\text{N}_8\text{F}_{12}\text{O}_4\text{P}_2\text{Ru}_2$: C, 45.72; H, 3.38; N, 8.54. Found: C, 45.62; H, 3.39; N, 8.51. Calc for $\text{C}_{60}\text{H}_{48}\text{N}_8\text{F}_{12}\text{O}_4\text{P}_2\text{Ru}_2$: C, 50.14; H, 3.37; N, 7.80. Found: C, 49.92; H, 3.40; N, 7.72. Calc for $\text{C}_{70}\text{H}_{52}\text{N}_8\text{F}_{12}\text{O}_4\text{P}_2\text{Ru}_2\cdot\text{H}_2\text{O}$: C, 53.23; H, 3.44; N, 7.10. Found: C, 53.32; H, 3.45; N, 6.97.

Preparation of [(bpy)₂RuL](PF₆) Mononuclear Compounds. All of the mononuclear compounds were prepared with the same general procedure used for the dinuclear species except that the ratio of [(bpy)₂RuCl₂] \cdot 2H₂O to L was 1:2. Purification of the crude materials was by the thin-layer method. A final recrystallization was from 1:5 $\text{CH}_3\text{CN}/\text{CH}_3\text{CH}_2\text{OH}$, as for the dinuclear materials. The pure materials were dried under vacuum. Anal. Calc for $\text{C}_{30}\text{H}_{29}\text{N}_4\text{F}_6\text{O}_4\text{PRu}$: C, 47.69; H, 3.87; N, 7.41. Found: C, 47.23; H, 3.93; N, 7.93. Calc for $\text{C}_{40}\text{H}_{33}\text{N}_4\text{F}_6\text{O}_4\text{PRu}$: C, 54.61; H, 3.78; N, 6.37. Found: C, 54.34; H, 3.86; N, 6.34. Calc for $\text{C}_{50}\text{H}_{37}\text{N}_4\text{F}_6\text{O}_4\text{PRu}$: C, 59.82; H, 3.71; N, 5.58. Found: C, 59.54; H, 3.77; N, 5.55.

Molecular Computations. Molecular mechanics calculations were performed with the CACHE suite of programs available from Tetraonix, version 2.8. This program starts with the MM2 force field developed by Allinger⁷ and augments it with a generalized force field for interactions not parametrized by MM2 for the entire periodic table. The energy terms for bond stretch, bond angle, dihedral angle, improper torsion, van der Waals electrostatics, and hydrogen bonding interactions are included in each calculation. All atoms are moved at least once during minimization. Optimization continues until the energy change is less than 0.001 kcal/mol. Each molecule was optimized to an energy minimum at least six times, each attempt beginning from a different and usually absurd starting geometry. Optimization was attempted by the methods of steepest descent, conjugate gradient, and block-diagonal Newton–Raphson. Only reproducible optimization obtained from several different attempts were considered to represent valid global minima.

Since our version of the ZINDO⁹ program on the CACHE system is restricted to 60 atoms and 210 basis functions, it was necessary to downsize the experimental systems. This was accomplished by using the molecules which had been optimized by molecular mechanics as described above and removing the nonbridging bipy ligands. The nitrogens in positions *trans* to the bridging oxygens were replaced with hydrides. The geometry of the $\text{Ru}^{\text{II}}\text{—L—Ru}^{\text{II}}$ system was then left intact

(4) (a) Hoffman, B. M.; Ratner, M. R. *J. Am. Chem. Soc.* **1987**, *109*, 6237. (b) Hoffman, B. M.; Ratner, M. R. *J. Am. Chem. Soc.* **1988**, *110*, 8267. (c) Brunshwig, B. S.; Sutin, N. *J. Am. Chem. Soc.* **1989**, *111*, 7454. (d) Natan, M. J.; Hoffman, B. M. *J. Am. Chem. Soc.* **1989**, *111*, 6468. (e) Natan, M. J.; Kuila, D.; Baxter, W. W.; King, B. C.; Hawkrige, F. M.; Hoffman, B. M. *J. Am. Chem. Soc.* **1990**, *112*, 4081. (f) Conrad, D. W.; Zhang, H.; Stewart, D. E.; Scott, R. A. *J. Am. Chem. Soc.* **1992**, *114*, 9909. (5) Sullivan, B. P.; Salmon, D. J.; Meyer, T. J. *Inorg. Chem.* **1978**, *17*, 3334.

(6) (a) Charles, R. G. *Org. Synth.* **1959**, *39*, 61. (b) Abell, R. D. *J. Chem. Soc.* **1912**, *101*, 989. (c) Cava, M. P.; Behforouz, M.; Husbands, G. E. M.; Srinivasan, M. *J. Am. Chem. Soc.* **1973**, *95*, 2561. (7) Allinger, N. L. *J. Am. Chem. Soc.* **1977**, *99*, 8127.

Table 1. Electronic and Spectral Data for the Mononuclear and Dinuclear Complexes

compd	$\Pi \rightarrow \Pi^*(1)^a$	$\Pi \rightarrow \Pi^*(2)^a$	$t \rightarrow \Pi^*(1)^a$	$t \rightarrow \Pi^*(2)^a$
[RuMe ₂ Me ₂ Ru]	293 (8.67)	245 (4.47)	512 (1.54)	373 (2.25)
[RuMe ₂ Ph ₂ Ru]	293 (9.50)	245 (5.35)	505 (1.76)	377 (2.22)
[RuPh ₂ Ph ₂ Ru]	293 (10.4)	245 (7.89)	502 (2.33)	366 (2.72)
[RuMe ₂ Me ₂]	293 (5.98)	245 (2.75)	510 (0.89)	371 (1.35)
[RuMe ₂ Ph ₂]	293 (5.77)	245 (3.12)	505 (0.85)	366 (1.39)
[RuPh ₂ Ph ₂]	293 (6.72)	245 (4.86)	498 (1.08)	329 (1.57)

^a All values given as λ_{\max} , nm ($10^{-4} \epsilon_{\max}$, M⁻¹ cm⁻¹).

by using ZINDO to minimize the energy of the resulting structure. The INDO/1 parametrization method of Pople⁸ was used in all calculations. The program has been augmented with additional spectroscopic and geometry parameters for first- and second-row transition metals. The restricted Hartree-Fock self-consistent field method was used to generate molecular orbitals in an iterative fashion. All distances are in angstroms with the differences in the last decimal place given in parentheses: Ru-Ru 8.095 for [RuMe₂Me₂Ru], 8.094 for [RuMe₂Ph₂Ru], and 7.961 for [RuPh₂Ph₂Ru]; Ru-H 1.994(1); Ru-O 1.97(1); C(acac)-C(Me) 1.51(1); C(acac)-C(Ph) 1.47(1); C-C in Ph ring 1.396(1); C-H in Ph ring 1.103(1); C(acac)-C(Me) 1.51(1). The C-C-C bond angles in the acac rings were as follows: [RuMe₂Me₂Ru], 120.0(1); [RuMe₂Ph₂Ru], 117.5(2); [RuPh₂Ph₂Ru], 113.1(2).

Analyses. All microanalyses were obtained from Atlantic Microlab Inc., Norcross, GA.

Results

Unlike the majority of reported ruthenium bipyridyl compounds, the fully reduced mononuclear and dinuclear compounds are all relatively stable both to light and to solvation processes. The spectra show no absorbance changes for at least 24 h. The mixed-valence and fully oxidized species are less stable and show absorbance decreases of 10–15% in 1 h at room temperature.

Electronic Spectra. The UV-vis spectra of the fully reduced binuclears show two major peaks which may be assigned to bipyridyl intraligand transitions. The bands at 293 nm and approximately 245 nm are labeled as $\pi \rightarrow \pi^*$ transitions by analogy to the work of Crutchley and Lever.¹⁰ The shoulder on the side of these bands can be ascribed to vibrational structure as well as to the splitting of the π and π^* orbitals of bipyridyl by interaction with the t_{2g} type orbitals of the metals. The peaks in the visible spectra are MLCT transition bands. The first set, which consists of two transitions, involves excitations to the lowest $\pi^*(bpy)$ level $t_2 \rightarrow \pi^*(1)$ and a second set approximately 6000 cm⁻¹ higher in energy involves transitions assigned as $t_2 \rightarrow \pi^*(2)$. The data for all the complexes are given in Table 1. Since the ligand field strength of the bridge ligand is weaker than that of a bpy ligand, the MLCT transitions in both the mononuclear and dinuclear series occurred at lower energy than those of the parent complex [Ru(bpy)₃]²⁺.

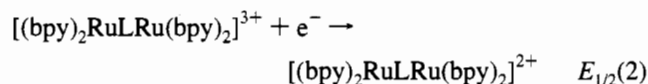
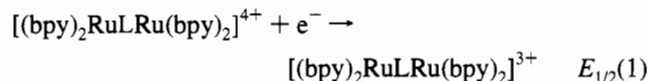
Electrochemistry. Cyclic voltammograms were obtained for all the mononuclear and dinuclear complexes. Variation of the scan rate showed no appreciable change in the peak position nor in the peak to peak separation. The two pairs of redox peaks

Table 2. Electrochemical Data for The Mononuclear and Dinuclear Complexes

compd	$E_{1/2}(1),^a$	$E_{1/2}(2),^a$	K_{com}
[RuMe ₂ Me ₂ Ru]	+640 (60)	+723 (60)	26
[RuMe ₂ Ph ₂ Ru]	+660 (60)	+775 (60)	89
[RuPh ₂ Ph ₂ Ru]	+660 (59)	+805 (59)	287
[RuMe ₂ Me ₂]		+680 (60)	
[RuMe ₂ Ph ₂]		+729 (60)	
[RuPh ₂ Ph ₂]		+719 (60)	

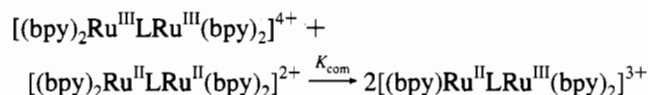
^a Values shown in parentheses are peak-to-peak separations. The concentration of each complex was 1×10^{-3} M in acetonitrile containing 0.1 M TBAH. Ferrocene under the same conditions gives +440 (59) mV.

correspond to two one-electron processes



where $\Delta E = E_{1/2}(1) - E_{1/2}(2)$. The electrochemical data are collected in Table 2.

The mixed-valence species comproportionates in solution to give some of the fully oxidized and some of the fully reduced species according to the following equilibrium:



The value of the comproportionation constant K_{com} is given in the usual fashion as

$$K_{\text{com}} = \frac{[\text{II,III}]^2}{[\text{II,II}][\text{III,III}]}$$

The comproportionation constant K_{com} generated in this fashion may be calculated from the electrochemical data using the equation¹¹

$$\log K_{\text{com}} = \Delta E/0.059$$

and the calculated values are collected in Table 2.

Near-Infrared Spectra. The spectra of all the binuclear ions in their [II,II], [II,III], and [III,III] oxidation states were recorded in CH₃CN and CD₃CN in a 2.0 cm quartz cell. None of the [II,II] and [III,III] ions showed any bands whereas all of the mixed-valence species, represented by [II,III] produced an intervalence transition (IT) band in this spectral region. There was no evidence of any bands in either oxidation state, II or III, of the monomers in the near-IR spectrum. Information on the IT bands for the mixed-valence species is given in Table 3. All extinction coefficients are corrected for the comproportionation equilibrium using the electrochemical data.

Assuming a Gaussian line shape on an energy scale and that the electron transfer process is adiabatic, the Marcus-Hush theory^{13,15,17a} can be employed to analyze the properties of the IT band. The bandwidth at half-height can be calculated from

- (8) Pople, J. A.; Beveridge, D. L.; Dobosh, P. A. *J. Chem. Phys.* **1967**, *47*, 2026.
 (9) (a) Ridley, J.; Zerner, M. C. *Theor. Chim. Acta* **1976**, *42*, 21. (b) Bacon, A. D.; Zerner, M. C. *Theor. Chim. Acta* **1979**, *42*, 21. (c) Zerner, M. C.; Loew, G. H.; Kirchner, R. F.; Mueller-Westerhoff, U. T. *J. Am. Chem. Soc.* **1980**, *102*, 589. (d) Anderson, W. P.; Cundarai, T. R.; Drago, R. S.; Zerner, M. C. *Inorg. Chem.* **1990**, *29*, 1.
 (10) Crutchley, R. J.; Lever, A. B. P. *Inorg. Chem.* **1982**, *21*, 2276.

- (11) Sutton, J. E.; Sutton, P. M.; Taube, H. *Inorg. Chem.* **1979**, *18*, 1017.
 (12) Hanch, C.; Leo, A.; Taft, R. W. *Chem. Rev.* **1991**, *91*, 165.
 (13) Hush, N. S. *Electrochim. Acta* **1968**, *13*, 1005.
 (14) Robin, M. B.; Day, P. *Adv. Inorg. Chem. Radiochem.* **1967**, *10*, 247.
 (15) (a) Marcus, R. A. *Annu. Rev. Phys. Chem.* **1964**, *15*, 155. (b) Marcus, R. A. *J. Chem. Phys.* **1965**, *43*, 679.
 (16) (a) Creutz, C. *Prog. Inorg. Chem.* **1983**, *30*, 1. (b) Sutin, N. *Prog. Inorg. Chem.* **1983**, *30*, 441.

Table 3. Spectral Data for the Intervalence Transition Band of the Dinuclear Mixed-Valence Species

compd	ν_{\max} , $\text{cm}^{-1} \times 10^3$	ϵ , $\text{M}^{-1} \text{cm}^{-1}$	$\Sigma\sigma_1$	$\nu_{1/2,\text{exp}}$, $\text{cm}^{-1} \times 10^3$	$\nu_{1/2,\text{cal}}$, $\text{cm}^{-1} \times 10^3$	$\nu_{1/2,\text{exp}}/\nu_{1/2,\text{cal}}$	$10^3\alpha^2$	H_{AB} , cm^{-1}
[RuMe ₂ Me ₂ Ru]	7.27	199	-0.04	5.73	4.10	1.39	1.0	230
[RuMe ₂ Ph ₂ Ru]	6.57	442	0.22	5.43	3.90	1.39	2.4	320
[RuPh ₂ Ph ₂ Ru]	5.24	1962	0.48	3.97	3.48	1.14	8.5	510

the following equation

$$\nu_{\max} = (\nu_{1/2})^2/2.31$$

where ν_{\max} is the energy of the optical IT band at its maximum in $\text{cm}^{-1} \times 10^3$ and $\nu_{1/2}$ is the bandwidth at half-height, also in $\text{cm}^{-1} \times 10^3$. Experimental values are obtained directly from the IT band spectra, and the results of the calculated and experimentally measured quantities are listed in Table 3. The experimental values are slightly larger than those calculated from the Hush theory but are close enough that the systems may be regarded as weakly coupled or belonging to the Robin and Day class II designation.¹⁴

The electron coupling matrix element H_{AB} is given by

$$H_{\text{AB}} = 2.05 \times 10^{-2} \sqrt{\frac{\epsilon_{\max}\nu_{1/2}}{\nu_{\max}}} \left(\frac{\nu_{\max}}{r}\right) \text{cm}^{-1}$$

The direct metal-to-metal distance, r , is measured in Å and ϵ_{\max} is the molar extinction coefficient ($\text{M}^{-1} \text{cm}^{-1}$) at ν_{\max} . Values of H_{AB} for our molecules are given in Table 3. A large compendium of values for similar systems has been given by Creutz.^{16a} They range from 50 to 900 cm^{-1} . The value calculated for the Meyer ion, [(bpy)₂ClRu(py₂)RuCl(py₂)₂]³⁺, where py₂ is pyrazine, is 400 cm^{-1} , which is comparable to the values reported for the series of compounds reported in the present paper.

The mixing coefficient α for the electronic wave functions may also be employed as a measure of delocalization between the metal centers and can be estimated from the following equation¹⁷

$$\alpha^2 = \frac{(2.05 \times 10^{-2})^2 \epsilon_{\max}\nu_{1/2}}{\nu_{\max}d^2}$$

where d is the internuclear separation between ruthenium atoms (in Å). Employing the value of 8.10 Å obtained in the molecular mechanics calculations for the binuclears, we calculated the α^2 values; the results are listed in Table 3. The values are all relatively small, indicating again that the metals are only weakly coupled electronically. For comparison the value calculated for the Meyer ion is 2.6×10^{-3} .

The energy of the IT band, E_{op} , was found to correlate satisfactorily with the log of its extinction coefficient, ϵ , taken at the peak maximum, and $\Delta E_{1/2}$ of the cyclic voltammograms, which is a measure of the extent of coupling between the metal centers. All of these parameters also correlated with the sum of the field/inductive substituent coefficients σ_1 as measured by Taft using ¹⁹F NMR spectrometry for the four substituents giving a quantitative structure-activity relationship (QSAR). In a recent review, Hansch, Leo, and Taft¹² compiled an enormous data base of these and many other substituent constants. The energy of the optical band for intervalence electron transfer was higher for the methyl than for the phenyl derivative, as might be expected from their respective inductive effects, and this is manifested by a change in electronic coupling between the metal centers. The correlation with σ_1 which we found implies that the only way the substituent can influence

the electron transfer process is through space (the field effect) and through the intervening σ bonds (the inductive effect). In other words, the resonance effects due to the conjugated π system are apparently constant in all three molecules.

Molecular Calculations. Molecular structures generated by molecular mechanics methods are shown in Figure 1. Although intuitively it might be expected that the two pentane-2,4-dione pseudoaromatic rings would obtain their greatest stability by adopting a position with each ring at right angles to the other, thus minimizing the steric constraints of their side chains, this did not happen in any of the structures. The dihedral angles, defined by the two bridging carbons and two carbons joined to them in a *trans* orientation, for the three structures were 31, 43, and 65° away from the expected 90° twist for the [RuMe₂Me₂Ru], [RuMe₂Ph₂Ru], and [RuPh₂Ph₂Ru] structures, respectively. These dihedral angles are found to correlate very well with the energy of the IT band as shown in Figure 2, suggesting that the spacial requirements of the structure are dictated by the need for maximal possible coupling between the metal centers. The benzenes and pyridyl rings of the bipyridine ligands can be clearly seen to line up in pairs for both the [RuMe₂Ph₂Ru] and [RuPh₂Ph₂Ru] structures. Figure 3 shows how this is accomplished with the [RuPh₂Ph₂Ru] complex having the pairs rotated *trans* to each other along the Ru-Ru axis and with the [RuMe₂Ph₂Ru] structure lining up with both phenyl/pyridyl pairs on the same side of the Ru-Ru axis. In the latter species, there will obviously be more room to accommodate all of the available rings close to each other.

There have been a few other studies on the effect of bond angles on electron transfer rates, and the subject has been treated in some detail by theoreticians. Hendrickson and his group¹⁸ have performed Huckel MO calculations on biferrocenium triiodide for different dihedral angles between the two cyclopentadiene rings to elucidate the geometric effect on the rates of intramolecular electron transfer in mixed-valence biferrocenium cations. They found a nonlinear decrease in the HOMO-LUMO gap as a function of tilt angle. As the cyclopentadiene rings were bent back, their π orbitals started to interact with the metal nonbonding orbitals. This increased the rate of intramolecular electron transfer. In 1990, Maruyama and Mataga and their co-workers¹⁹ examined a series of diporphyrins separated by aromatic spacer molecules. One porphyrin had a Zn atom in its center and the other had an Fe(II) moiety which allowed photoexcited electron transfer to occur. They found that the rates of charge separation depended only on distance and were unaffected by orientation of the intervening spacers whereas the rates of charge recombination were independent of both distance (from 8 to 23 Å) and orientation. The charge recombination was therefore considered unlikely to involve an intersite electron transfer process but was instead attributed to a localized reaction such as a charge of ligation. In 1991, McLendon²⁰ reported the first systematic study of bis(porphyrin) complexes by the same photoexcited mechanism which did show a bond angle dependency. He prepared a series of complexes

(17) (a) Hush, N. S. *Prog. Inorg. Chem.* **1967**, *8*, 391. (b) Callahan, R. W.; Brown, G. M.; Meyer, T. J. *Inorg. Chem.* **1975**, *14*, 1443.

(18) Hendrickson, D. N.; Oh, S. M.; Dong, T.-Y.; Kambara, T.; Cohn, M. J.; Moore, M. F. *Comments Inorg. Chem.* **1985**, *4*, 329.

(19) Osuka, A.; Maruyama, K.; Mataga, N.; Asahi, T.; Yamazaki, I.; Tamai, N. *J. Am. Chem. Soc.* **1990**, *112*, 4958.

(20) Helms, A.; Heiler, D.; McLendon, G. *J. Am. Chem. Soc.* **1991**, *113*, 4325.

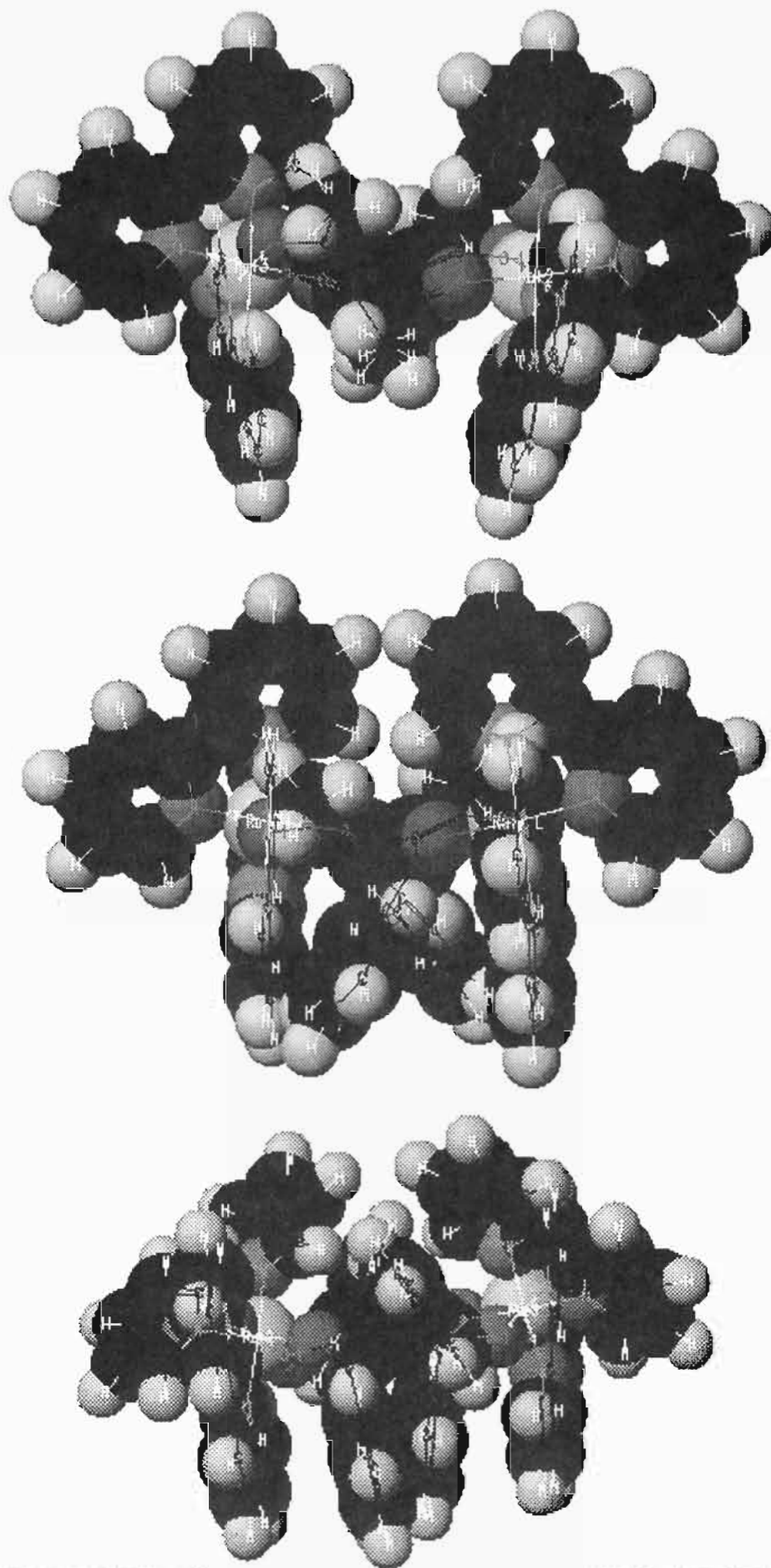


Figure 1. Energy-minimized structures generated by molecular mechanics: (top) [RuMe₃Me₃Ru]; (middle) [RuMe₂Ph₂Ru]; (bottom) [RuPh₂Ph₂Ru].

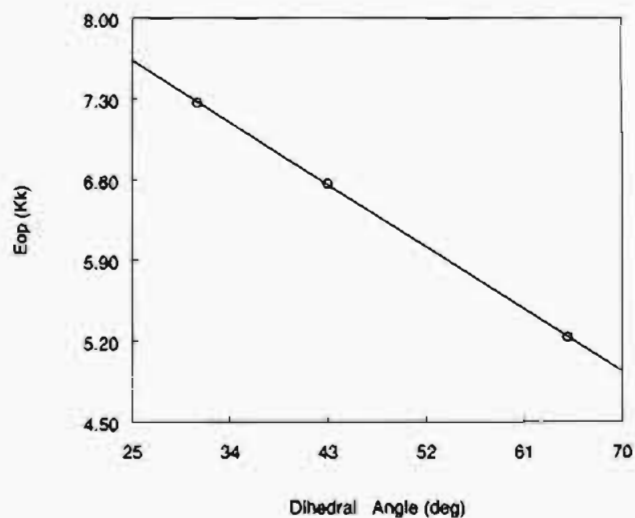


Figure 2. Plot of the dihedral angles defining the twist in the orientation of the two pseudoaromatic pentane-2,4-dione rings with respect to each other versus the energy of the IT band. The dihedral angles were measured from the energy-optimized molecular mechanics structures.

of the type porphyrin–diphenyl–porphyrin which had known bond angles. The angle between the porphyrin ring and the

adjacent phenyl ring is rigidly constrained to 90° by the nonbonded contacts between the phenyl protons and the alkyl substituents in the flanking rings. Thus the overall porphyrin–porphyrin dihedral angle is determined by the torsional angle, θ , between the two phenyl rings of the bridge. Simple symmetry arguments would suggest that the rate at 90°, for which the rings are perpendicular to each other, should be much slower than that at 0°, for which the phenyl rings are coplanar. Surprisingly, maximum rates were found at both 0 and 90° and a minimum rate occurred at 45°. This unexpected result was actually predicted by Cave, Siders, and Marcus^{21b} in 1984 since the porphyrin π orbitals are antisymmetric with respect to the porphyrin plane and therefore the only way to obtain π overlap between the phenyl bridge and the porphyrin ring is to employ antisymmetric combinations of the wave functions of the bridge. Rotating from 0 to 90°, the bonding combination becomes antibonding and vice versa so that similar overlap occurs at 0 and 90° but the $|H_{AB}|$ approaches 0 at the intermediate position, 45°. McLendon²² later reported a weak distance dependence having $\beta = 0.4 \text{ \AA}^{-1}$ for a series of related bridged polyphenyls. They concluded that the rate dropoff was due primarily to the break in conjugation which occurs at each phenyl junction due to the twist angle of about 50°.

The ZINDO calculations produce molecular orbitals which

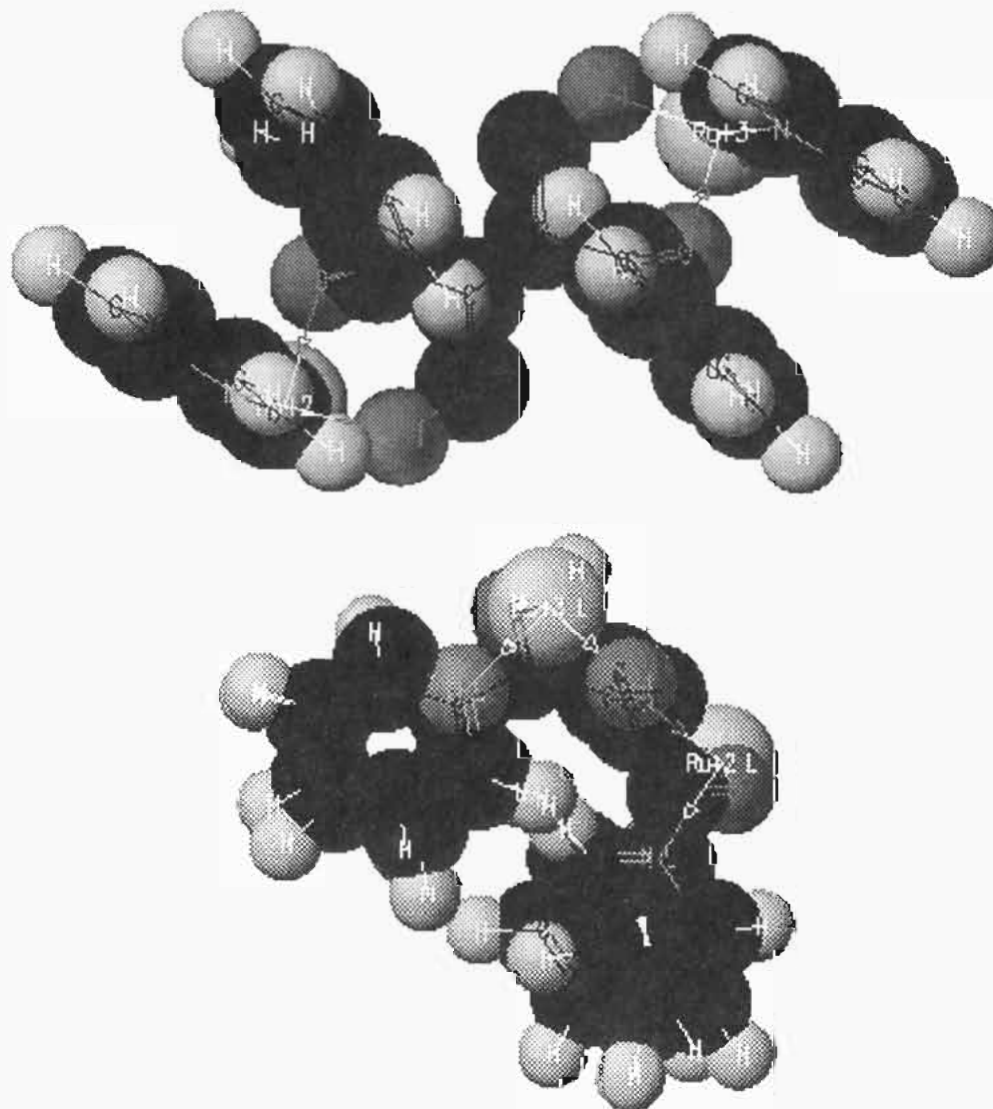


Figure 3. Views showing the orientation of the benzene rings with respect to each other: (top) [RuMe₂Ph₂Ru] structure; (bottom) [RuPh₂Ph₂Ru] structure. All pyridyl rings except those “twinned” to the phenyl rings have been removed from the top structure for clarity, and all bipyridyl ligands have been removed from the bottom structure.

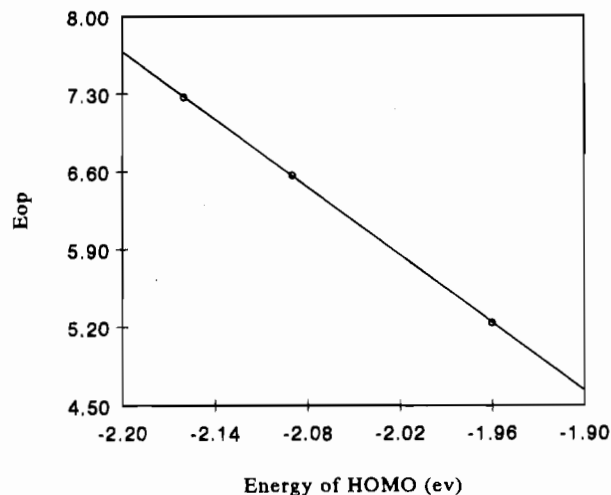


Figure 4. Plot of the energy of the IT band and the HOMO bond energy calculated by the ZINDO method.

show no obvious interactions between the phenyl rings as one would expect from an examination of the structures generated by molecular mechanics. It might be anticipated, however, that the phenyl/pyridyl and/or pyridyl/pyridyl through-space interactions could form part of the electronic pathway between the two metal centers. This possibility obviously cannot be evaluated from the present calculations. It is generally believed for proteins, for example, that electron transfer occurs from the edge of a porphyrin ring. An excellent correlation was observed between the energy of the optical band and the HOMO band energy which might be expected for a superexchange (through-bond) mechanism (see Figure 4). We are unable to determine if similar nodal dependencies might be operating in our system as predicted for the aromatic spacers by Cave, Siders, and Marcus²¹ and observed by McLendon *et al.*²⁰ since none of our systems permit observation of the bond angles 0 and 90°.

Discussion

Model compounds have long been employed to try to obtain information on electron pathways in a more controlled setting than can be achieved in macromolecules such as proteins. For example, in 1982 we published^{3c} a paper on the following spiro ruthenium binuclears



where $n = 0-2$.

We noted that expected correlations were much better when we used the through-bond distances for this series of compounds rather than the direct metal-metal distance, which was the only distance parameter believed to be of importance by theoreticians at that time. We later published^{3d} a through-bond electron transfer pathway based on molecular orbital calculations on the bridging ligands.

In the Meyer ion, $[(bpy)_2ClRu(py)_2RuCl(bpy)_2]^{3+}$, the Ru-Ru distance is approximately 6.8 Å and the electron coupling parameter, H_{AB} , is calculated to be 400 cm^{-1} . Our series of molecules are similar to this compound in that the spectator ligands are all bipyridines and the electron density from the metal atoms tends to be delocalized into these ligand orbitals. The Ru-Ru through-space distance in the present series is approximately 8.0 Å and H_{AB} varies from 230 to 510 cm^{-1} , values which are quite comparable to that produced by the very simple pyrazine bridging ligand, although the distance is a little longer. The complexes choose to orient themselves with parallel phenyl/phenyl and phenyl/pyridyl rings by changing the dihedral angle of the bridging group at the expense of maximizing the space they could occupy which would require a dihedral angle of 90°. This suggests that a strong through-space component of the electronic coupling exists even for the pyridyl rings in the $[RuMe_2Me_2Ru]$ complex. An alternative explanation is that the geometry selected maximizes the inductive effects of the substituents. Finally, through-space and inductive effects may both be important with each having similar geometric constraints. The good correlation given by the ZINDO calculations which ignores the contribution of the pyridyl ligands but conserves the geometry of the bridging ligands argues for a predominantly inductive mechanism. Our work also indicates that information on the side chains themselves such as QSAR relationships may be useful either alone or as an additional variable within another mathematical model in helping to quantify the role of the intervening matter in assisting electron transfer processes in small molecules and perhaps also in proteins. We are currently constructing other models which are designed to separate the inductive and through-space components of the electronic pathways in an effort to address the questions raised in the present research.

Acknowledgment. We are grateful to the National Science Foundation for a Career Award Grant to N.A.L. and to CAChe Scientific for the generous gift of CAChe software which made this work possible.

IC940713G

- (21) (a) Cave, R. J.; Siders, P.; Marcus, R. A. *J. Phys. Chem.* **1986**, *90*, 1436. (b) Siders, P.; Cave, R. J.; Marcus, R. A. *J. Chem. Phys.* **1984**, *81*, 5613. (c) Ohta, K.; Closs, G. L.; Morokuma, K.; Green, N. J. *J. Am. Chem. Soc.* **1986**, *108*, 1319. (d) Paddon-Row, M. N.; Shephard, M. J.; Jordan, K. D. *J. Am. Chem. Soc.* **1993**, *115*, 3312.
- (22) Helms, A.; Heiler, D.; McLendon, G. *J. Am. Chem. Soc.* **1992**, *114*, 6227.